LETTER • OPEN ACCESS

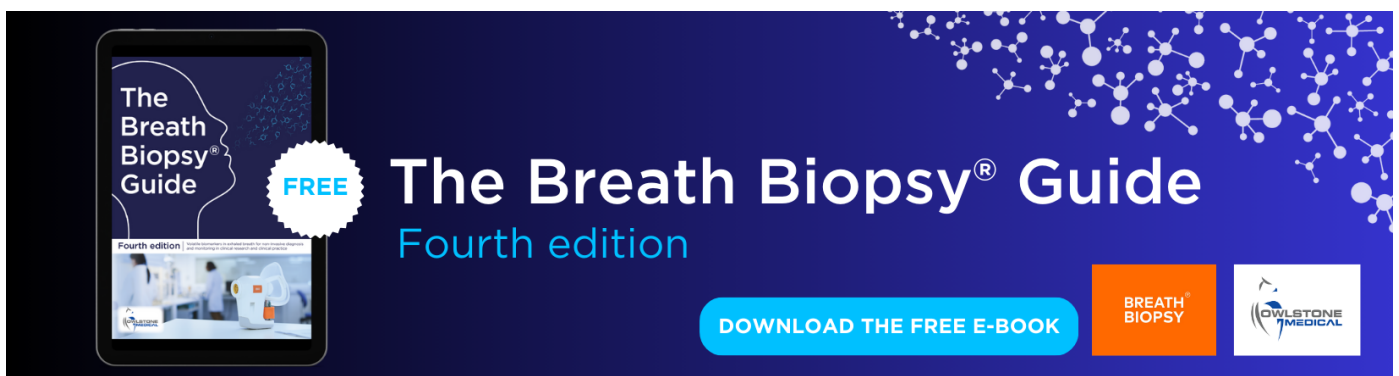# Climate-driven land surface phenology advance is overestimated due to ignoring land cover changes

View the article online for updates and enhancements.

ENVIRONMENTAL RESEARCH
LETTERS

CrossMark

LETTER

Climate-driven land surface phenology advance is overestimated due to ignoring land cover changes

Yuhao Pan[1,2,3], Dailiang Peng[1,2,*], Jing M Chen[4], Ranga B Myneni[5], Xiaoyang Zhang[6],
Alfredo R Huete[7], Yongshuo H Fu[8], Shijun Zheng[1], Kai Yan[9], Le Yu[10], Peng Zhu[11], Miaogen Shen[12],
Weimin Ju[13], Wenquan Zhu[14], Qiaoyun Xie[7], Wenjiang Huang[1,2], Zhengchao Chen[15], Jingfeng Huang[16]
and Chaoyang Wu[17]

1   Key Laboratory of Digital Earth Science, Aerospace Information Research Institute, Chinese Academy of Sciences, Beijing 100094, People's Republic of China
2   International Research Center of Big Data for Sustainable Development Goals, Beijing 100094, People's Republic of China
3   University of Chinese Academy of Sciences, Beijing 100049, People's Republic of China
4   Department of Geography and Program in Planning, University of Toronto, Toronto, ON M5S 3G3, Canada
5   Department of Earth and Environment, Boston University, Boston, MA 02215, United States of America
6   Geospatial Sciences Center of Excellence (GSCE), Department of Geography, South Dakota State University, Brookings, SD 57007, United States of America
7   University of Technology Sydney, Faculty of Science, Sydney, NSW 2007, Australia
8   College of Water Sciences, Beijing Normal University, Beijing 100875, People's Republic of China
9   School of Land Science and Techniques, China University of Geosciences, Beijing 100083, People's Republic of China
10   Ministry of Education Key Laboratory for Earth System Modeling, Department of Earth System Science, Tsinghua University, Beijing 100084, People's Republic of China
11   School of Geography and Planning, Sun Yat-Sen University, Guangzhou 510006, People's Republic of China
12   State Key Laboratory of Earth Surface Processes and Resource Ecology, Faculty of Geographical Science, Beijing Normal University, Beijing 100875, People's Republic of China
13   International Institute for Earth System Science, Nanjing University, Nanjing 210023, People's Republic of China
14   Institute of Remote Sensing Science and Engineering, Faculty of Geographical Science, Beijing Normal University, Beijing 100875, People's Republic of China
15   Airborne Remote Sensing Center, Aerospace Information Research Institute, Chinese Academy of Sciences, Beijing 100094, People's Republic of China
16   Institute of Applied Remote Sensing and Information Technology, Zhejiang University, Hangzhou 310058, People's Republic of China
17   The Key Laboratory of Land Surface Pattern and Simulation, Institute of Geographical Sciences and Natural Resources Research, Chinese Academy of Sciences, Beijing 100101, People's Republic of China
*   Author to whom any correspondence should be addressed.

E-mail: pengdl@aircas.ac.cn

Abstract

Global warming has led to earlier spring green-up dates (GUDs) in recent decades with significant consequences for global carbon and hydrologic cycles. In addition to changes in climate, land cover change (LCC), including interchanges between vegetation and non-vegetation, and among plants with different functional traits, may also affect GUD. Here, we analyzed how satellite-derived GUD from 1992 to 2020 was impacted by changes in temperature, precipitation, standardized precipitation evapotranspiration index (SPEI), solar radiation, and LCC for the Northern Hemisphere ($>30°$ N). While the climate variables had larger impact overall, variability in GUD was controlled by LCC for 6% of the Northern Hemisphere, with systematically earlier or later changes among transitions between different land cover types. These changes were found mainly along the southeastern coast of the United States, in Central-north Europe, and across northeastern China. We further showed that climate change attribution of earlier GUD during 1992–2020 was overestimated by three days when the impact of LCC was ignored. Our results deepen the understanding of how LCC impacts GUD variability and enables scientists to more accurately evaluate the impact of climate change on land surface phenology.

1. Introduction

Plant phenology, especially spring green-up date (GUD), is highly sensitive to climate change (Richardson *et al* 2013) yet also impacts climate and terrestrial ecosystems processes, forming a feedback loop (Richardson *et al* 2013, Piao *et al* 2019a, 2019b). Consequently, research has increasingly focused on the effects of climate change on phenology (Richardson *et al* 2013, Piao *et al* 2019a). Advancing GUD based on satellite data has been revealed by recent researches, which is closely related to warming, light period, and CO_2 fertilization (Richardson *et al* 2013, Piao *et al* 2019a). Numerous studies of both *in situ* and satellite-derived phenology have shown that the earlier onset of GUD in the Northern Hemisphere is, in part, a result of global warming (Forkel *et al* 2014, Keenan 2015). The complex relationship between GUD and climate variables has been observed. For example, preseason maximum temperature and winter precipitation had great influence on GUD (Piao *et al* 2015), chilling days and light period also had a considerable impacts on GUD trend (Fu *et al* 2015). In addition, except climate change, the GUD trend also varied at different altitudes (Vitasse *et al* 2018). The causes of GUD changes are complex that include climate change and land cover change (LCC). LCC can change the energy balance and biogeochemical cycles, further affecting surface characteristic (such as GUD) (Duveiller *et al* 2018). Therefore, quantifying changes in phenology and LCC impacts is of prime importance when analyzing climate change impacts and accurately estimating ecosystem carbon flux.

Mechanisms surrounding this trend in GUD are complex. The GUD is closely related to temperature, precipitation, and radiation (Richardson *et al* 2013, Piao *et al* 2019a). Warmer spring temperatures decrease the amount of time required to meet a species' growing degree day (GDD) requirement for green-up to begin. However, temperature effects are strongly modulated by winter precipitation (Forkel *et al* 2014, Fu *et al* 2014, Yun *et al* 2018). An increase in winter precipitation falling as snow may increase the time it takes vegetation to meet the GDD requirement, especially in temperature-limited ecosystems (Yun *et al* 2018). Solar radiation also influences GUD because it partly represents photoperiod (daylength) (Richardson *et al* 2013, Piao *et al* 2019a) and itself may be affected by precipitation (Tang *et al* 2016). For example, more solar radiation usually means higher surface temperature and a long photoperiod, and promotes earlier GUD (Richardson *et al* 2013, Tang *et al* 2016). In addition, climate change impacts on GUD vary with elevation, vegetation type, and tree age. Changes in advancing GUD vary with elevation as stronger trends are found at higher elevation, likely caused by faster preseason warming in these locations over time (Piao *et al* 2011, Vitasse *et al* 2018).

Despite considerable effort, the mechanistic understanding of GUD dynamics and its drivers is incomplete. In addition to the parameters listed previously, LCC exerts a significant impact on land surface phenology change. Grasslands usually have earlier GUD than forests because grasslands require fewer GDD than forests (Ganguly *et al* 2010, Jeganathan *et al* 2014), while the GUD for trees becomes later as they age because older trees require more GDD than younger ones (Menzel and Fabian 1999). Case studies on intensive agricultural areas (Zhang *et al* 2019) and burned forest areas (Wang and Zhang 2017, 2020) have highlighted the essential role of LCC in understanding the spatial and interannual variations in land surface phenology widely associated with climate change. Studies have shown that the long-term trend in GUD for intensively cultivated areas is influenced by LCC and climate change, and the influence of LCC on GUD dominates in some regions (Zhang *et al* 2019). For example, the GUD was delayed before an area burned but that now it occurs earlier and has advanced by ∼15 days (Wang and Zhang 2017). However, the quantitative contribution of LCC to changes in GUD has not been systematically studied.

The earth's land surface has changed as a result of urbanization, afforestation, and cropland abandonment in the Northern Hemisphere during the past few decades and similar changes will continue into the future (Winkler *et al* 2021). Satellite-derived phenology provides an indication of current climate change from regional to global scales (Piao *et al* 2019a, Peng *et al* 2021). In particular, satellite-derived GUD have been widely employed to investigate warming impacts on promoting earlier GUD because of its wide coverage and long, continuous time-series. However, the spatial resolution of satellite-derived phenology used in global climate change studies is coarse (e.g. 500 m × 500 m or 0.05° × 0.05°). Phenology derived using coarse resolution LCC data may be incorrect because of the mixed pixel effect (Zhang *et al* 2017, Peng *et al* 2017b, 2018, 2021, Chen *et al* 2018). When analyzing interannual variation in satellite-derived phenology, many factors contribute to the final value assigned to each pixel, including LCC, climate, and other factors. To identify the effects of climate change on changes in GUD, we must first determine the impact of LCC (Richardson *et al* 2013, Helman 2018, Zhang *et al* 2019).

To determine the impact of LCC, we used long-term satellite-derived GUD and land cover data to characterize the LCC impacts on GUD for the period 1992–2020 in the Northern Hemisphere (>30° N). We examined the statistical relationships between the GUD and several parameters

(temperature, precipitation, radiation, standardized precipitation evapotranspiration index (SPEI) and LCC). Finally, trends in GUD were attributed proportionally to these different drivers.

2. Materials and methods

2.1. Satellite-derived GUD
The GUD data were derived from Global Long-Term Climate Modeling Grid Land Surface Phenology (CMGLSP, 1992–2016, 0.05°) (Zhang 2015), and VIIRS/NPP Land Surface Phenology Collection 2 (VNP22C2, 2013–2020, 0.05°) (Zhang *et al* 2020). Phenology metrics from CMGLSP and VNP22C2 were retrieved using a hybrid piecewise logistic model (Zhang *et al* 2003, 2018, Peng *et al* 2017c). We validated the consistency between CMGLSP and VNP22C2 for the period 2013–2016 when both datasets were available. We calculated the following to test numeric correlation: root mean square errors (RMSEs), Pearson correlation coefficient (*R*, ranging from −1 to 1) and agreement coefficient (AC, ranging from 0 to 1) (Ji and Gallo 2006). To test for spatial pattern consistency, we used the spatial efficiency metric (SPAEF, ranging from 0 to 1) (Koch *et al* 2018). The definitions and equations of these indices can be found in supplementary section 1. A higher value of *R*, AC, and SPAEF indicates a stronger numeric correlation and spatial consistency between the two datasets. The *R* and SPAEF were both greater than 0.9, AC was greater than 0.85, and RMSE was smaller than 13 days, indicating that numeric correlation and spatial patterns were consistent for the two datasets (supplementary figure S1). As a result, a GUD dataset for the period 1992–2020 was generated by combining CMGLSP for the period 1992–2016 with VNP22C2 for the period 2017–2020 with no further changes.

2.2. Climate data
Changes in GUD are highly associated with climate variables from preceding months (Piao *et al* 2015). We defined preseason as the period from 1 November of the preceding year to mean GUD (1992–2020) (Piao *et al* 2015). The ERA5-land reanalysis dataset provides a continuous hourly record of global land surface variables at 0.1° resolution since 1950 (Muñoz-Sabater *et al* 2021). We converted hourly to daily by taking the maximum of temperature, the sum of precipitation, and the average of radiation, within a day. We selected three climate variables generated by ERA5-land and calculated a preseason value for each year for the following variables: average maximum temperature (TMP, an average of all days maximum temperature, unit: °C), precipitation (PRE, a sum of all days precipitation, unit: mm), radiation (RAD, an average of all days downward radiation, unit: W m^{-2}). We also utilized monthly

composite ERA5-land precipitation and potential evapotranspiration data to calculate SPEI in order to analyze the impact of drought on GUD. The timescale for SPEI was set at six months, and we chose the SPEI value for the 4th month of each year to represent the preseason drought conditions for that year. Climate variables were resampled to a resolution of 0.05° using bilinear interpolation to match the resolution of the GUD data.

2.3. Land cover data
We used European Space Agency Climate Change Initiative Land Cover (ESA CCI LC) data with 300 m resolution for the period 1992–2020 to investigate the impacts of LCC on the GUD trend. The ESA CCI LC provides continuous and annually updated global land cover products from 1992 to 2020 with 37 United Nations Land Cover Classification System (UNLCCS) classes. These data can be used as inputs for climate models as well as for scientific research such as forest and desertification monitoring and LCC monitoring (Hollmann *et al* 2013). Errors in land cover classification may be larger than LCC itself. Data production processes for ESA CCI LC ensured that each change persisted for more than two successive years to reduce false change detections (Li *et al* 2018). Because of irrigation and human management, changes in cropland are difficult to correlate with GUD, so we masked permanent cropland pixels for the period 1992–2020 to reduce error. We calculated a coefficient of variability based on the 37 land cover class fractions within each 0.05° × 0.05° grid using equation (1) to represent LCC year by year

$$ \text{LCC} = \frac{S}{|\bar{x}|} \tag{1} $$

where *S* and $\bar{x}$ are the standard deviation and mean value of the 37 land cover class fractions within a 0.05° × 0.05° grid.

2.4. Analyses
We used multiple linear regression to explore the effects of TMP, PRE, SPEI, RAD, and LCC on GUD (Le Provost *et al* 2020). The beta coefficients were interpreted as the single standard deviation change in the dependent variable caused by a single standard deviation change in the independent variable (Le Provost *et al* 2020). These coefficients were estimated using the ordinary least square method shown in equation (2):

$$ Y = \sum_{i=1}^{n} \beta_i x_i + \varepsilon \tag{2} $$

where *Y* is GUD, x_i is normalized independent variable, β_i is beta coefficient.

The relative contribution of each independent variable is defined as the corresponding percent of beta coefficient to the sum of all beta

Table 1. Rules to determine the effect of relative contribution. A positive relative contribution indicates that changes of the independent variable causes delaying GUD, a negative relative contribution indicates that changes of the independent variable causes advancing GUD.

Sign of beta coefficient	Sign of Thiel–Sen's slope	Sign of relative contribution
+	+	+(delaying)
	−	−(advancing)
−	+	−(advancing)
	−	+(delaying)

coefficients. Compare to slope detected by simple linear regression, slope from Thiel–Sen estimator is more robust for effect of outlier removal. Therefore, the sign of relative contribution was jointly determined by the sign of corresponding Thiel–Sen's slope and beta coefficient (table 1). A positive coefficient indicates that an increase in the independent variable delays GUD, while a negative coefficient indicates that an increase in the independent variable advances GUD. We defined the dominant driving factor for each grid as the variable with the largest beta coefficient.

To identify the signal of GUD changes due to each individual LCC from 1992 to 2020, a ridge-regression method was introduced to unravel the effect of each LCC on GUD (Huang *et al* 2020). To facilitate interpretation of LCC, the 37 UNLCCS classes were aggregated into the International Geosphere–Biosphere Programme (IGBP) classes using the crosswalk established in other studies (Duveiller *et al* 2018, Huang *et al* 2020). A set of 5-by-5 moving windows was used to decompose GUD changes resulting from the mix of the possible LCCs. For window *i*, a model was built using IGBP classes fractions of each of the 25 grids of the window as shown in equation (3)

$$y_i = X_i\beta_i + \varepsilon_i, i = 1, 2, \ldots, N \tag{3}$$

where X_i is an explanatory variable matrix containing the fractions of all land cover classes in each of the 25 grids in the window; y_i is a vector containing 25 GUD values; β_i is the vector of the regression coefficients; and ε_i is the vector of the model residual. The model is then solved using ridge-regression.

Finally, multiple year mean matrices were obtained for the period 1992–2020 describing changes in land cover transitions and the corresponding standard errors using established methods (Huang *et al* 2020). The number of GUD changes misinterpreted by LCC was defined as the product of LCC's relative contribution and the change in GUD for the period 1992–2020.
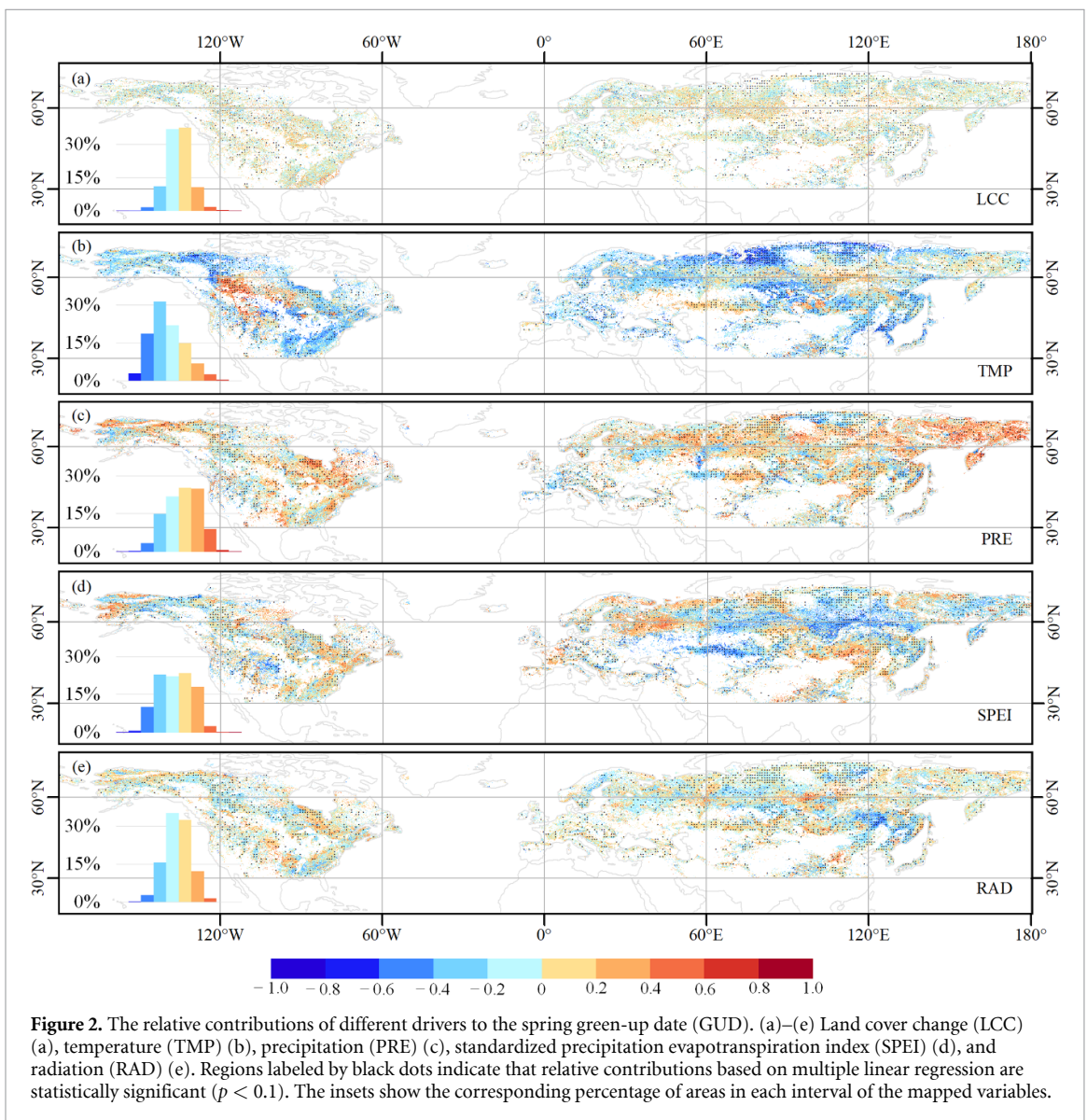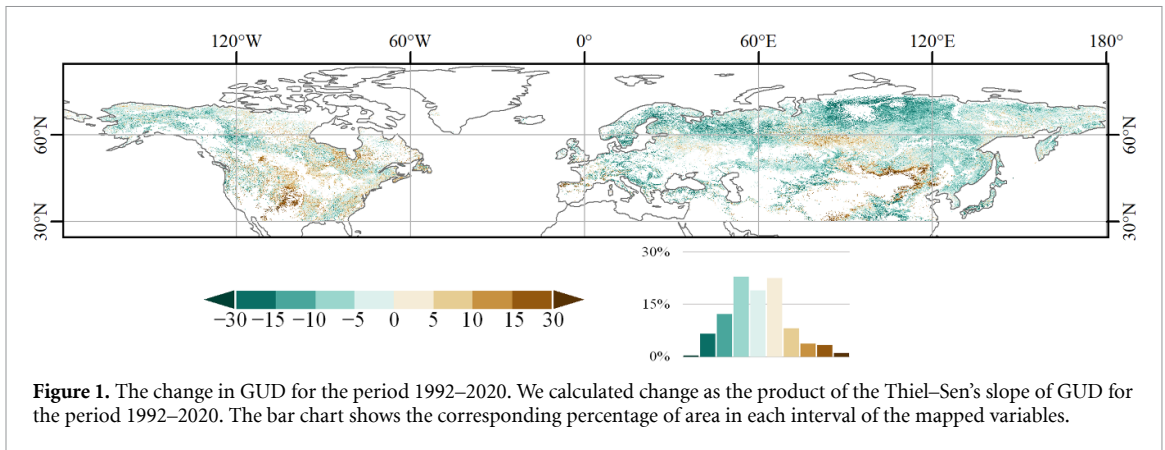
3. Results

3.1. Relative contribution of LCC, temperature, precipitation, SPEI, and radiation to changes in GUD

Between 1992 and 2020 the GUD started 5–15 days earlier for 35% of the area, and it was mainly found in areas above 60° N and across most of Europe. About 7% of the area in Eastern Europe and Central Russia showed GUD starting 15–30 days earlier. The GUD was delayed for 39% of the land area found in central North America, northern China, and regions between 80° E–100° E and 50° N–60° N (figure 1).
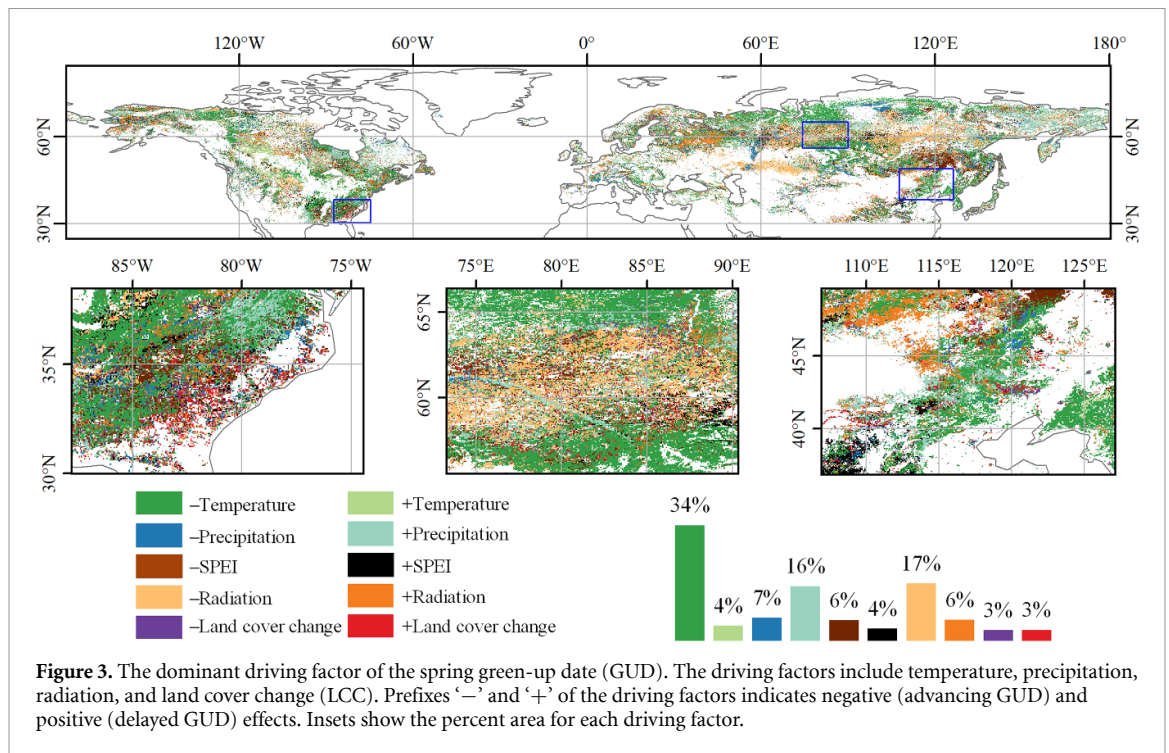
We estimated LCC as coefficient of variability of land cover class fractions within each 0.05° × 0.05° grid, then, linear statistical relationships between GUD and LCC, temperature, precipitation, SPEI and radiation were analyzed (section 2), revealing that the effects of these drivers on GUD varies regionally. The LCC delayed GUD across 50% area, which was mainly found in west-central Russia (50° E–90° E, 55° N–65° N), the southeastern coast of the United States and the Great Lakes region (figure 2(a)). The relative contribution of LCC ranged from 0% to 20% across 37% of the area (figure 2(a)). Temperature advanced GUD in 75% area, with 22% of that area having a relative contribution greater than 40% (figure 2(b)). Only 25% of the area had a delayed GUD response to temperature—primarily in Central America (120° W–90° W, 45° N–60° N) (figure 2(b)). Precipitation delayed GUD across more than 60% of the area, mainly above 60° N, and 25% of the area had a relative contribution between 20% and 40% (figure 2(c)). The area of advanced GUD caused by precipitation was mainly distributed across parts of Central Asia with a dry or semi-dry climate (figure 2(c)). The area of advanced GUD caused by SPEI changes was mainly found in Central Asia and Russia (figure 2(d)). Radiation's spatial contribution was generally opposite that of precipitation. For example, radiation advanced GUD in Northeast China while precipitation delayed GUD (figures 2(c) and (e)).

Based on the annual trends of GUD and various driving factors during different time periods, significant differences were found between 1992–2000, 2001–2010, and 2011–2020. TMP, PRE and SPEI increased most rapidly during 2011–2020, while GUD, LCC decreased most rapidly during 2011–2020. It can be concluded that the period of 2011–2020 was the period during which LCC and other climatic variables had the greatest impact on GUD (see supplementary section 2 and figures S2–S9). After analyzing the impact of LCC, TMP, PRE, SPEI, and RAD on GUD changes along latitude, altitude, and precipitation gradient, several patterns were identified. Specifically, LCC was found to cause GUD

Figure 1. The change in GUD for the period 1992–2020. We calculated change as the product of the Thiel–Sen's slope of GUD for the period 1992–2020. The bar chart shows the corresponding percentage of area in each interval of the mapped variables.

Figure 2. The relative contributions of different drivers to the spring green-up date (GUD). (a)–(e) Land cover change (LCC) (a), temperature (TMP) (b), precipitation (PRE) (c), standardized precipitation evapotranspiration index (SPEI) (d), and radiation (RAD) (e). Regions labeled by black dots indicate that relative contributions based on multiple linear regression are statistically significant ($p < 0.1$). The insets show the corresponding percentage of areas in each interval of the mapped variables.

to delay in the latitude range of 30°–40° N and to advance in the latitude range of 60°–70° N, with a higher relative contribution at altitudes above 4000 m. An increase in SPEI mainly caused GUD to advance when the precipitation was less than 1000 mm, but caused GUD to delay when the precipitation exceeded 2000 mm (see supplementary section 3 and figure S10).

Figure 3. The dominant driving factor of the spring green-up date (GUD). The driving factors include temperature, precipitation, radiation, and land cover change (LCC). Prefixes '−' and '+' of the driving factors indicates negative (advancing GUD) and positive (delayed GUD) effects. Insets show the percent area for each driving factor.

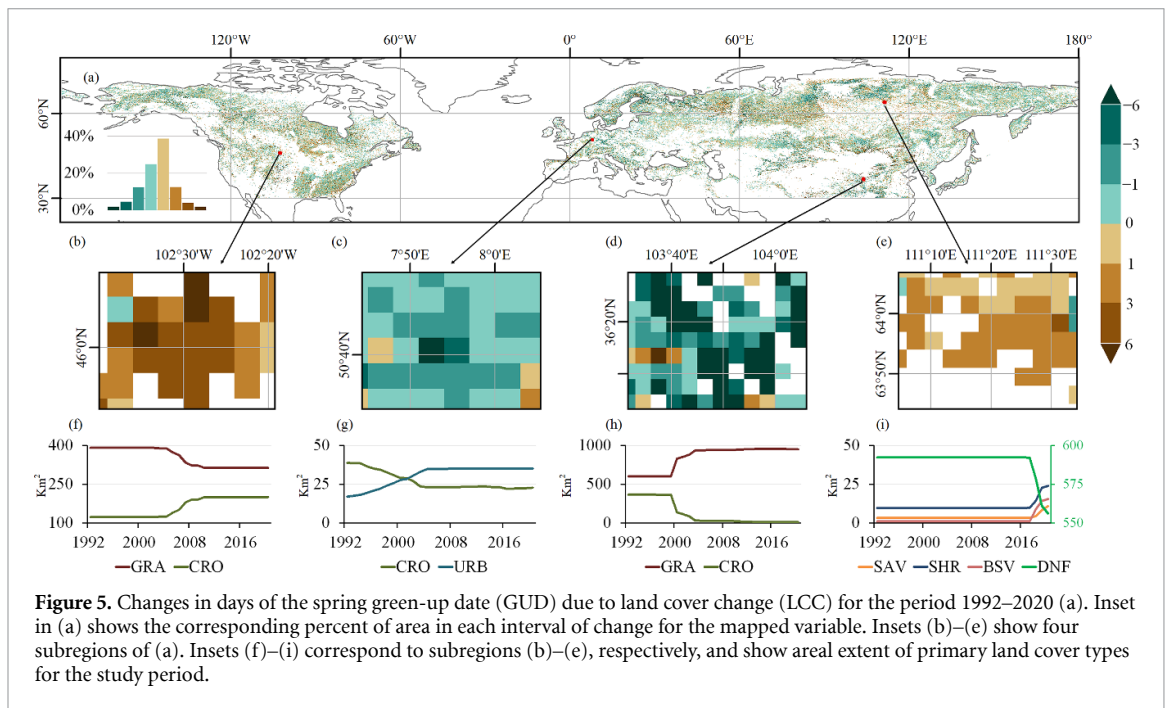### 3.2. LCC impact on changes in GUD is non-negligible

The factor with the greatest relative contribution to each grid was defined as the dominant factor (section 2), and the area influenced predominantly by LCC accounted for 6% of the total study area. The contribution of LCC to interannual variation in GUD was considerable in Northeast China, along the southeastern coast of the United States, and throughout Central Russia. Temperature, precipitation, SPEI, and radiation had greater impacts on interannual changes in GUD overall, being the dominant factor in 38%, 23%, 10% and 23% of the area, respectively (figure 3). Advancing GUD dominated by temperature accounted for about 25% of the area and was mainly distributed above 60° N, while delayed GUD was mainly found in Central America (120° W–90° W, 45° N–60° N), accounting for about 4% of the area. Delayed GUD resulting primarily from precipitation was mainly distributed across Central Russia (90° E–110° E, 60° N–65° N), accounting for about 3% area. Advancing GUD dominated by SPEI was mainly distributed across Central Asia (50° E–80° E, 45° N–50° N and 100° E–120° E, 60° N–65° N), accounting for about 9% of the area. Advancing GUD dominated by radiation was mainly located in Northeast China (110° E–130° E, 45° N–55° N), accounting for about 4% of the area.

3.3. Characteristics of changes in GUD for specific LCC

Using methods from a previous study (Huang *et al* 2020), we identified GUD changes caused by transition between individual land cover types. We filtered

the data for illogical land cover transitions (Peng *et al* 2017a), such as transformations from deciduous broadleaf forests into evergreen needleleaf forests in a single year. As shown in figure 4, the GUD changes induced by individual LCC varied greatly. Some transition types did not occur (e.g. transition from cropland or urban areas to shrublands), so changes in GUD could not be identified. The transitions from deciduous broadleaf forests, savannas, croplands or wetlands to other land cover types usually caused advancing GUD, with transitions from deciduous broadleaf forests, savannas and wetlands to urban areas advancing GUD by about ten days, eight days, and seven days, respectively. The transition from deciduous needleleaf forests or urban areas to other land cover types usually delayed GUD, with transitions from deciduous needleleaf forests to grasslands and urban areas to sparse vegetation inducing a change of about four days and five days, respectively. Changes in GUD between individual land cover types had opposite responses (Duveiller *et al* 2018). Therefore, reforestation of deciduous needleleaf forests or urban expansion usually advanced GUD, while deforestation and urban reduction delayed GUD. Similarly, cropland expansion often delayed GUD, while cropland reduction had the opposite effect.

The land cover transition matrix for the period 1992–2020 reveals that about 8% of the area underwent land cover transitions, which is comparable to the 6% of the area whose dominant driver of GUD change was LCC. The two land cover types that decreased most were evergreen needleleaf forests (1.5%) and bare/sparse vegetation (0.99%). The two

Figure 4. Decomposition of spring green-up date changes for individual land cover transitions. Changes are from the land cover type labeled in each box to the different land cover types in columns with colors. (e.g. DBF to SAV, and SAV to WET).

Figure 5. Changes in days of the spring green-up date (GUD) due to land cover change (LCC) for the period 1992–2020 (a). Inset in (a) shows the corresponding percent of area in each interval of change for the mapped variable. Insets (b)–(e) show four subregions of (a). Insets (f)–(i) correspond to subregions (b)–(e), respectively, and show areal extent of primary land cover types for the study period.

land cover types that increased most were savannas (1.53%) and croplands (1.28%). The three land cover transitions seen most often were evergreen needleleaf forests to savannas, grasslands to croplands, and deciduous needleleaf forests to savannas, which were 0.47%, 0.38% and 0.36%, respectively. These three primary land cover transitions delayed GUD two days, three days, and four days per year, respectively, which is one reason why the percent of LCC that delayed GUD was higher than the percent of LCC that advanced GUD.

3.4. Climate change impact on advancing GUD was overestimated

The GUD changes induced by LCC are shown in figure 5(a). The average advanced (3.0 days) and delayed (3.3 days) LCC-driven GUD changes from 1992 to 2020 accounted for about 22% and 15% of corresponding GUD changes, respectively (figure 6). The average advanced (13.6 days) climate (including temperature, precipitation, SPEI and radiation)-driven GUD changes from 1992 to 2020 accounted for 81% of corresponding GUD changes, respectively
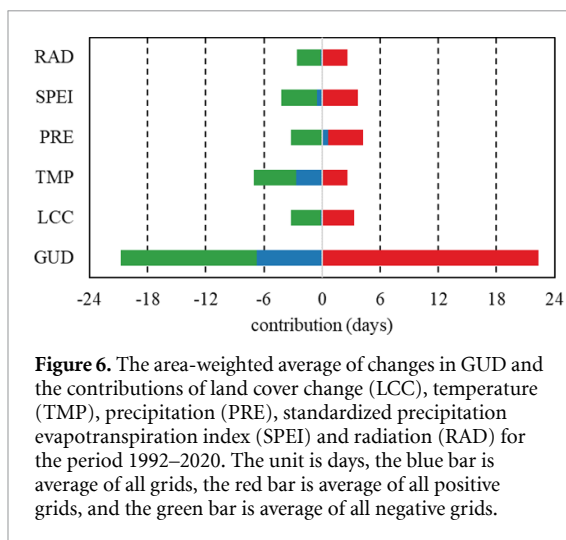
Figure 6. The area-weighted average of changes in GUD and the contributions of land cover change (LCC), temperature (TMP), precipitation (PRE), standardized precipitation evapotranspiration index (SPEI) and radiation (RAD) for the period 1992–2020. The unit is days, the blue bar is average of all grids, the red bar is average of all positive grids, and the green bar is average of all negative grids.

(figure 6). The distribution of LCC-driven GUD changes was uniform. Overall, LCC delayed GUD in about 57% of the area, with 6% of the area delayed by more than one to three days. On the other hand, LCC advanced GUD in about 43% of the area, with 12% advancing one to three days (figure 5(a)). Regions with noticeable LCC-driven GUD changes were located mainly along the southeastern coast of the United States, in Central-northern Europe, and in Northeastern China (120° E–135° E, 45° N–50° N) with about seven days, six days, and nine days advancing GUD, respectively. We selected four sub-regions to verify if GUD changes caused by LCC agreed with the results shown in figure 4. In these four sub-regions, urban and cropland expansion were the major drivers of GUD change. In the sub-regions shown in figures 5(b) and (d), the main LCC was the transition between grassland and cropland, thereby delaying and advancing GUD, respectively. In the sub-region shown in figure 5(c), the main transition was urban expansion (figure 5(g)), which advanced GUD. In the sub-region shown in figure 5(e), the main change in LCC was deciduous needle leaf forest deforestation (figure 5(i)), which delayed GUD.

4. Discussion and conclusions

4.1. Validation of calculated GUD trends

In this study, on average, GUD advanced 1.1 days per decade in the Northern Hemisphere from 1992 to 2020. A previous study showed that GUD for the Northern Hemisphere advanced on average 2.1 days per decade for the period 1982–2011 (Piao *et al* 2019a). A second study revealed that the rate of change in GUD per 1 °C of warming decreased by half when comparing the period 1999–2013 to that of 1980–1994 (Fu *et al* 2015). In addition, advancing GUD trends observed in most of Europe and half of North America (figure 1) were consistent with results of yet another study that used different methods

to calculate GUD (Huang *et al* 2017). In a qualitative assessment, this demonstrates that the GUD data used in this study are able to capture similar phenology dynamics to those identified by others.

4.2. The role of climate

Temperature is considered to be a primary factor controlling changes in GUD, and previous studies observed that maximum temperature had a greater influence on GUD changes than minimum temperature (Piao *et al* 2015, Fu *et al* 2016), which is why we selected average preseason maximum temperature. We also confirmed that recent warming has led to advancing GUD (Tang *et al* 2016, Piao *et al* 2019a) (figure 2(b)), which is shown by the negative correlation between temperature and GUD in the Northern Hemisphere (figure 7(b)). Precipitation plays a co-dominant role with temperature in land surface phenology dynamics (Forkel *et al* 2014). At latitudes above 50° N, increased preseason precipitation usually delays GUD, showing a positive correlation (figures 2(c) and 7(c)). In mountain areas and in cold regions, e.g. continental northern regions (>50° N), increased precipitation may occur partly as snow (Shutova *et al* 2006). Increased snow cover in spring may melt later and delay GUD (Shutova *et al* 2006, Tang *et al* 2016). On the other hand, increased water supply in spring can advance GUD in warm regions (Shutova *et al* 2006). Moreover, increased preseason precipitation can be accompanied by more cloud cover, which reduces the amount of incoming shortwave radiation (Shutova *et al* 2006). Heavy clouds can moderate surface temperatures and decrease solar radiation, both of which would delay GUD (Shutova *et al* 2006, Richardson *et al* 2013, Tang *et al* 2016). The partial correlations between GUD and both precipitation and radiation were opposite in sign (figures 7(c) and (e)), indicating that increased preseason precipitation accompanied by heavy cloud cover may mitigate the impacts of reduced radiation on GUD. In addition, the impacts of drought on GUD changes is also considerable, extreme drought events will cause delaying GUD and the alleviation of drought will cause advancing GUD (Li *et al* 2023), which is shown by negative correlation between SPEI and GUD in Central Asia and Central east Russia and 6% area with advancing GUD predominated by SPEI changes (figures 7(d) and (3)).

4.3. The role of LCC

Different land cover types have different phenological characteristics (Ganguly *et al* 2010, Jeganathan *et al* 2014). For example, the GUD of urban vegetation occurs earlier than that of other surrounding vegetation types (Meng *et al* 2020). Because of the mixed pixel effect in land surface phenology (Chen *et al* 2018), a coarse grid—such as the 0.05° grid used in this study—invariably includes several vegetation
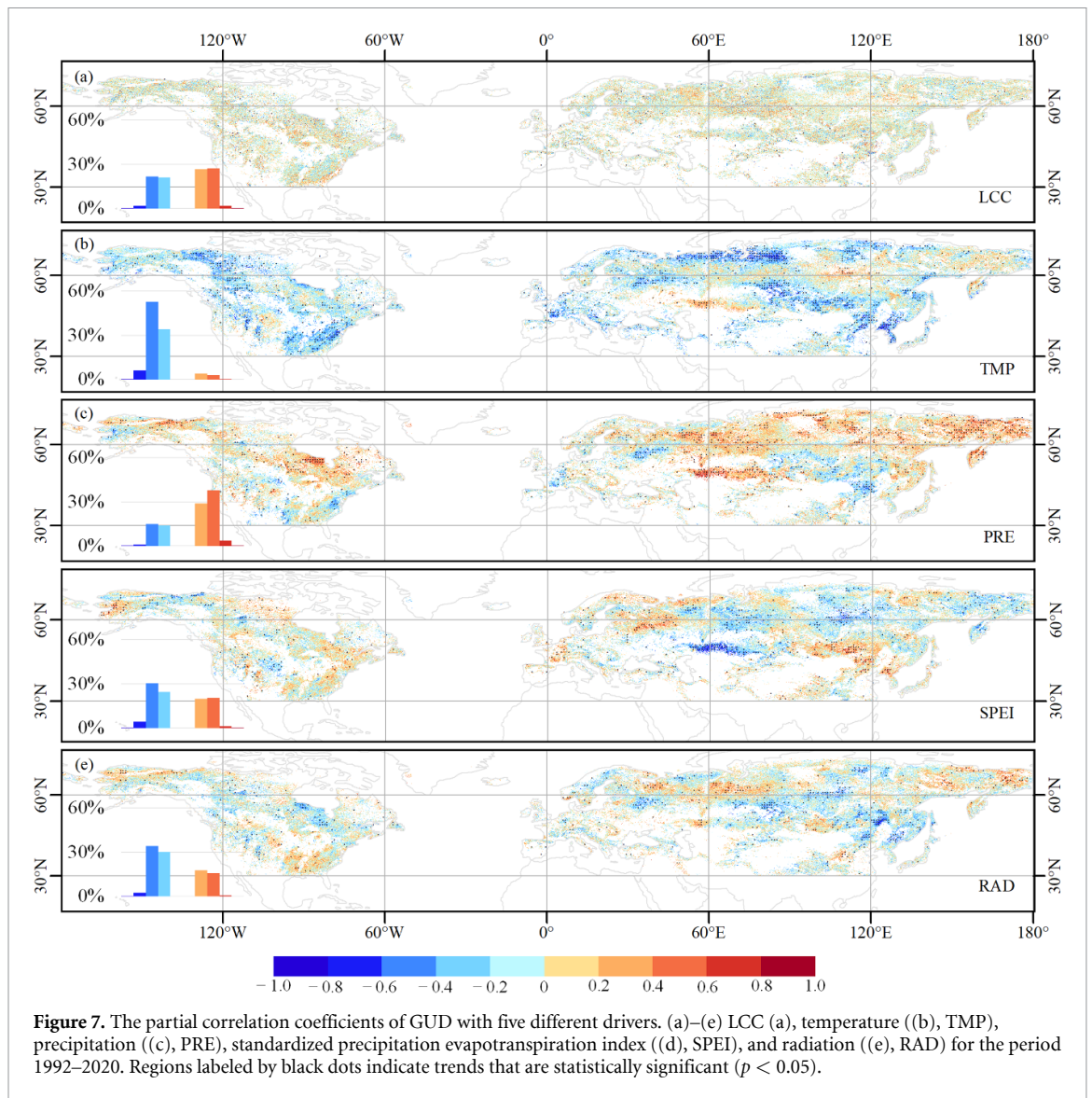
Figure 7. The partial correlation coefficients of GUD with five different drivers. (a)–(e) LCC (a), temperature ((b), TMP), precipitation ((c), PRE), standardized precipitation evapotranspiration index ((d), SPEI), and radiation ((e), RAD) for the period 1992–2020. Regions labeled by black dots indicate trends that are statistically significant ($p < 0.05$).

types. Interannual variation in vegetation composition would change GUD (Peng *et al* 2017b, Helman 2018), and this change is not caused by climate change. Changes in land cover type also result in changes in surface radiation budget and physiological characteristics that affect the local climate and energy balance (Duveiller *et al* 2018), thus altering phenology, which have been evidenced by negative correlation between temperature and GUD changes caused by land cover transitions (figure 4 and supplement figure S11). For example, the conversion of forest to shrub in burned area after a forest fire causes GUD to change from a delaying to an advancing trend (Wang and Zhang 2017), which agrees with our results that deforestation of deciduous needleleaf forests advances GUD. The mechanism for this change is the rapid increase in surface albedo and concomitant decrease in evaporation that usually results from the transition from boreal forest to shrub or grassland, which eventually manifests as a drop in temperature in the middle and high latitudes of the Northern

Hemisphere (Duveiller *et al* 2018), thus delaying GUD. Moreover, the temperature of urban areas is higher than that of surrounding rural areas, causing GUD to occur earlier in urban vegetation (Li *et al* 2017, Meng *et al* 2020, Tian *et al* 2020). Therefore, urban expansion usually leads to advancing GUD (figure 5(c)).

4.4. Possible future research

Nitrogen deposition impacts vegetation growth by affecting soil fertility, soil acid–base balance, and nitrogen concentration in leaves (Pan *et al* 2009, Wu *et al* 2014). Studies have shown an advanced budding time in response to increased nitrogen deposition in Tibet (Xi *et al* 2015), and nitrogen deposition contributed to 30.5% of interannual variations in the autumn phenology (Guo *et al* 2021). The indirect effects of budding time and autumn phenology on GUD (Richardson *et al* 2013, Tang *et al* 2016, Piao *et al* 2019a) and the effect of nitrogen deposition on constraining plant phenology need further exploration.

The atmospheric CO_2 concentration mainly influences vegetation photosynthesis and reproductive phenophases (Shen *et al* 2022); however, the mechanism of the impact of increasing CO_2 on GUD is still controversial. There are two possible hypotheses: one is that sufficient CO_2 during vegetation growth enhances frost resistance in vegetation the next year, and the other is that increased CO_2 partly alleviates the negative effects of warming on water availability (Piao *et al* 2019a). In addition to the effects of nitrogen deposition and CO_2 fertilization on GUD, the ecological impact of invariants in land cover are also worth studying as, for example, forest age and changes in crop cultivar also affect GUD (Menzel and Fabian 1999, Rezaei *et al* 2018).

We found that LCC may overestimate GUD by 3.3 days (even more than 10 days in some regions). Given that increased carbon sinks due to advance of GUD, could mitigate the risk of climate change to a limited extent (Piao *et al* 2019b; Chen 2021), the question arises as to whether LCC could offset the beneficial effects of GUD advancement. In terms of relevance for society, the findings of this study may be important for land management and policy formulation. Understanding the role of LCC in shaping the growing season can help inform decisions that may impact carbon uptake and ecosystem services.

In conclusion, by analyzing the statistical relationships between GUD and the individual parameters including temperature, precipitation, radiation, and LCC, we found that LCC exerts a non-negligible impact on GUD. More than 6% of the area with significant GUD change is controlled by LCC. The effect of climate change is overestimated by at least 22% (i.e. 3.3 days) from 1992 to 2020 when LCC is ignored. Our results enrich the understanding of how LCC impacts GUD, allowing us to better understand the climate-driven changes in GUD.

Data availability statement

The data that support the findings of this study are available upon reasonable request from the authors.

Acknowledgments

ORCID iDs

Yuhao Pan ⬤ https://orcid.org/0000-0002-5384-4624

Xiaoyang Zhang ⬤ https://orcid.org/0000-0001-8456-0547

Alfredo R Huete ⬤ https://orcid.org/0000-0003-2809-2376

Yongshuo H Fu ⬤ https://orcid.org/0000-0002-9761-5292

Shijun Zheng ⬤ https://orcid.org/0000-0002-8034-5011

Le Yu ⬤ https://orcid.org/0000-0003-3115-2042

Qiaoyun Xie ⬤ https://orcid.org/0000-0002-1576-6610

References

Chen J 2021 Carbon neutrality: toward a sustainable future *The Innovation* **2** 100127

Chen X, Wang D, Chen J, Wang C and Shen M 2018 The mixed pixel effect in land surface phenology: a simulation study *Remote Sens. Environ.* **211** 338–44

Duveiller G, Hooker J and Cescatti A 2018 The mark of vegetation change on Earth's surface energy balance *Nat. Commun.* **9** 679

Forkel M, Carvalhais N, Schaphoff S, V. Bloh W, Migliavacca M, Thurner M and Thonicke K 2014 Identifying environmental controls on vegetation greenness phenology through model–data integration *Biogeosciences* **11** 7025–50

Fu Y H *et al* 2015 Declining global warming effects on the phenology of spring leaf unfolding *Nature* **526** 104–7

Fu Y H, Liu Y, De Boeck H J, Menzel A, Nijs I, Peaucelle M, Peñuelas J, Piao S and Janssens I A 2016 Three times greater weight of daytime than of night-time temperature on leaf unfolding phenology in temperate trees *New Phytol.* **212** 590–7

Fu Y H, Piao S, Zhao H, Jeong S-J, Wang X, Vitasse Y, Ciais P and Janssens I A 2014 Unexpected role of winter precipitation in determining heat requirement for spring vegetation green-up at northern middle and high latitudes *Glob. Change Biol.* **20** 3743–55

Ganguly S, Friedl M A, Tan B, Zhang X and Verma M 2010 Land surface phenology from MODIS: characterization of the Collection 5 global land cover dynamics product *Remote Sens. Environ.* **114** 1805–16

Guo M, Wu C, Peng J, Lu L and Li S 2021 Identifying contributions of climatic and atmospheric changes to autumn phenology over mid-high latitudes of Northern Hemisphere *Glob. Planet. Change* **197** 103396

Helman D 2018 Land surface phenology: what do we really 'see' from space? *Sci. Total Environ.* **618** 665–73

Hollmann R *et al* 2013 The ESA climate change initiative: satellite data records for essential climate variables *Bull. Am. Meteorol. Soc.* **94** 1541–52

Huang B, Hu X, Fuglstad G-A, Zhou X, Zhao W and Cherubini F 2020 Predominant regional biophysical cooling from recent land cover changes in Europe *Nat. Commun.* **11** 1066

Huang M *et al* 2017 Velocity of change in vegetation productivity over northern high latitudes *Nat. Ecol. Evol.* **1** 1649–54

Jeganathan C, Dash J and Atkinson P M 2014 Remotely sensed trends in the phenology of northern high latitude terrestrial vegetation, controlling for land cover change and vegetation type *Remote Sens. Environ.* **143** 154–70

Ji L and Gallo K 2006 An agreement coefficient for image comparison *Photogramm. Eng. Remote Sens.* **73** 823–33

Keenan T F 2015 Phenology: spring greening in a warming world *Nature* **526** 48–49

Koch J, Demirel M C and Stisen S 2018 The SPAtial EFficiency metric (SPAEF): multiple-component evaluation of spatial patterns for optimization of hydrological models *Geosci. Model Dev.* **11** 1873–86

Le Provost G, Badenhausser I, Le Bagousse-Pinguet Y, Clough Y, Henckel L, Violle C, Bretagnolle V, Roncoroni M,

Manning P and Gross N 2020 Land-use history impacts functional diversity across multiple trophic groups *Proc. Natl Acad. Sci.* **117** 1573–9

Li W, MacBean N, Ciais P, Defourny P, Lamarche C, Bontemps S, Houghton R A and Peng S 2018 Gross and net land cover changes in the main plant functional types derived from the annual ESA CCI land cover maps (1992–2015) *Earth Syst. Sci. Data* **10** 219–34

Li X, Zhou Y, Asrar G R, Mao J, Li X and Li W 2017 Response of vegetation phenology to urbanization in the conterminous United States *Glob. Change Biol.* **23** 2818–30

Li Y *et al* 2023 Widespread spring phenology effects on drought recovery of Northern Hemisphere ecosystems *Nat. Clim. Change* **13** 182–8

Meng L *et al* 2020 Urban warming advances spring phenology but reduces the response of phenology to temperature in the conterminous United States *Proc. Natl Acad. Sci.* **117** 4228–33

Menzel A and Fabian P 1999 Growing season extended in Europe *Nature* **397** 659

Muñoz-Sabater J *et al* 2021 ERA5-Land: a state-of-the-art global reanalysis dataset for land applications *Earth Syst. Sci. Data* **13** 4349–83

Pan Y, Birdsey R, Hom J and McCullough K 2009 Separating effects of changes in atmospheric composition, climate and land-use on carbon sequestration of U.S. Mid-Atlantic temperate forests *For. Ecol. Manage.* **259** 151–64

Peng D L, Zhang X, Wu C, Huang W, Gonsamo A, Huete A R, Didan K, Tan B, Liu X and Zhang B 2017c Intercomparison and evaluation of spring phenology products using National Phenology Network and AmeriFlux observations in the contiguous United States *Agric. For. Meteorol.* **242** 33–46

Peng D *et al* 2017b Scaling effects on spring phenology detections from MODIS data at multiple spatial resolutions over the contiguous United States *ISPRS J. Photogramm. Remote Sens.* **132** 185–98

Peng D *et al* 2021 Investigation of land surface phenology detections in shrublands using multiple scale satellite data *Remote Sens. Environ.* **252** 112–33

Peng D, Wu C, Zhang X, Yu L, Huete A R, Wang F, Luo S, Liu X and Zhang H 2018 Scaling up spring phenology derived from remote sensing images *Agric. For. Meteorol.* **256–257** 207–19

Peng D, Zhang B, Wu C, Huete A R, Gonsamo A, Lei L, Ponce-Campos G E, Liu X and Wu Y 2017a Country-level net primary production distribution and response to drought and land cover change *Sci. Total Environ.* **574** 65–77

Piao S *et al* 2015 Leaf onset in the Northern Hemisphere triggered by daytime temperature *Nat. Commun.* **6** 6911

Piao S *et al* 2019b Characteristics, drivers and feedbacks of global greening *Nat. Rev. Earth Environ.* **1** 14–27

Piao S, Cui M, Chen A, Wang X, Ciais P, Liu J and Tang Y 2011 Altitude and temperature dependence of change in the spring vegetation green-up date from 1982 to 2006 in the Qinghai-Xizang Plateau *Agric. For. Meteorol.* **151** 1599–608

Piao S, Liu Q, Chen A, Janssens I A, Fu Y, Dai J, Liu L, Lian X, Shen M and Zhu X 2019a Plant phenology and global climate change: current progresses and challenges *Glob. Change Biol.* **25** 1922–40

Rezaei E E, Siebert S, Hüging H and Ewert F 2018 Climate change effect on wheat phenology depends on cultivar change *Sci. Rep.* **8** 4891

Richardson A D, Keenan T F, Migliavacca M, Ryu Y, Sonnentag O and Toomey M 2013 Climate change, phenology, and phenological control of vegetation feedbacks to the climate system *Agric. For. Meteorol.* **169** 156–73

Shen M *et al* 2022 Plant phenology changes and drivers on the Qinghai–Tibetan Plateau *Nat. Rev. Earth Environ.* **3** 633–51

Shutova E, Wielgolaski F E, Karlsen S R, Makarova O, Berlina N, Filimonova T, Haraldsson E, Aspholm P E, Flø L and Høgda K A 2006 Growing seasons of Nordic mountain birch in northernmost Europe as indicated by long-term field studies and analyses of satellite images *Int. J. Biometeorol.* **51** 155–66

Tang J, Körner C, Muraoka H, Piao S, Shen M, Thackeray S J and Yang X 2016 Emerging opportunities and challenges in phenology: a review *Ecosphere* **7** e01436

Tian J, Zhu X, Wu J, Shen M and Chen J 2020 Coarse-resolution satellite images overestimate urbanization effects on vegetation spring phenology *Remote Sens.* **12** 117

Vitasse Y, Signarbieux C and Fu Y H 2018 Global warming leads to more uniform spring phenology across elevations *Proc. Natl Acad. Sci. USA* **115** 1004–8

Wang J and Zhang X 2017 Impacts of wildfires on interannual trends in land surface phenology: an investigation of the Hayman Fire *Environ. Res. Lett.* **12** 054008

Wang J and Zhang X 2020 Investigation of wildfire impacts on land surface phenology from MODIS time series in the western US forests *ISPRS J. Photogramm. Remote Sens.* **159** 281–95

Winkler K, Fuchs R, Rounsevell M and Herold M 2021 Global land use changes are four times greater than previously estimated *Nat. Commun.* **12** 2501

Wu C, Hember R A, Chen J M, Kurz W A, Price D T, Boisvenue C, Gonsamo A and Ju W 2014 Accelerating forest growth enhancement due to climate and atmospheric changes in British Colombia, Canada over 1956–2001 *Sci. Rep.* **4** 4461

Xi Y, Zhang T, Zhang Y, Zhu J, Zhang G and Jiang Y 2015 Nitrogen addition alters the phenology of a dominant alpine plant in northern Tibet *Arct. Antarct. Alp. Res.* **47** 511–8

Yun J, Jeong S-J, Ho C-H, Park C-E, Park H and Kim J 2018 Influence of winter precipitation on spring phenology in boreal forests *Glob. Change Biol.* **24** 5176–87

Zhang X Y *et al* 2017 Exploration of scaling effects on coarse resolution land surface phenology *Remote Sens. Environ.* **190** 318–30

Zhang X 2015 Reconstruction of a complete global time series of daily vegetation index trajectory from long-term AVHRR data *Remote Sens. Environ.* **156** 457–72

Zhang X *et al* 2020 VIIRS/NPP land cover dynamics yearly L3 Global 0.05 Deg CMG V001 *NASA EOSDIS Land Processes DAAC* (https://doi.org/10.5067/VIIRS/VNP22C2.001)

Zhang X, Friedl M A, Schaaf C B, Strahler A H, Hodges J C F, Gao F, Reed B C and Huete A 2003 Monitoring vegetation phenology using MODIS *Remote Sens. Environ.* **84** 471–5

Zhang X, Liu L and Henebry G M 2019 Impacts of land cover and land use change on long-term trend of land surface phenology: a case study in agricultural ecosystems *Environ. Res. Lett.* **14** 044020

Zhang X, Liu L, Liu Y, Jayavelu S, Wang J, Moon M, Henebry G M, Friedl M A and Schaaf C B 2018 Generation and evaluation of the VIIRS land surface phenology product *Remote Sens. Environ.* **216** 212–29